

New fundamental parameters of the Galactic open clusters Berkeley 26, Czernik 27, Melotte 72, NGC 2479 and BH 37

Andrés E. Piatti^{1*} Juan J. Clariá^{2*} and Andrea V. Ahumada^{2,3*}

¹*Instituto de Astronomía y Física del Espacio, CC 67, Suc. 28, 1428, Ciudad de Buenos Aires, Argentina*

²*Observatorio Astronómico, Universidad Nacional de Córdoba, Laprida 854, 5000 Córdoba, Argentina*

³*European Southern Observatory, Alonso de Córdova 3107, Santiago, Chile*

7 November 2018

ABSTRACT

We have obtained CCD $UBVI_{KC}$ photometry down to $V \sim 21.0$ for the open clusters Berkeley 26, Czernik 27, Melotte 72, NGC 2479 and BH 37. The latter has never been studied before. Cluster stellar density profiles were obtained from star counts in appropriate-sized boxes distributed throughout the entire observed fields. Based on different measured indices, we estimate the ages of Berkeley 26, Melotte 72 and NGC 2479. On the other hand, we indicate possible solutions for the cluster fundamental parameters by matching theoretical isochrones which reasonably reproduce the main cluster features in their CMDs. In the case of NGC 2479, the cluster $E(B - V)$ and $E(V - I)$ colour excesses and apparent distance modulus were estimated from the fit of the Zero-Age Main Sequence (ZAMS) to the colour-colour and colour-magnitude diagrams, respectively.

Key words: Galaxy: open clusters and associations: general - open clusters and associations: individual: Berkeley 26 - open clusters and associations: individual: Czernik 27 - open clusters and associations: individual: Melotte 72 - open clusters and associations: individual: NGC 2479 - open clusters and associations: individual: BH 37 - Galaxy: general - techniques: photometric

1 INTRODUCTION

Besides the intrinsic interest in open clusters (OCs) in their own right, it is generally accepted that these objects are fundamental landmarks to probe the Galactic disk properties (see, e.g., Friel 1995). They are among the very few Galactic objects for which meaningful distances can be derived over a large range, which makes them an essential tool to constrain Galactic evolution theories. They also make it possible to derive more accurate ages than are possible with other disk objects. Therefore, the study of the Galactic OC system proves very useful to clarify the many queries concerning the assessment of chemical abundance gradients in the disk (see, e.g., Twarog, Ashman & Anthony-Twarog 1997; Chen, Hou & Wang 2003), Galactic structure and evolution (e.g., Janes & Adler 1982; Janes & Phelps 1994), interactions between thin and thick disks (e.g., Sandage 1988), as well as theories of stellar formation and evolution (e.g., Meynet, Mermilliod & Maeder 1993; Phelps & Janes 1993).

The OC catalogue by Lyngå (1987) includes 1700 entries. However, very little is known about many of them, except for their positions and approximate values of their angular sizes. At present, fewer than half of the known OCs have been studied in detail to derive their fundamental parameters. The current paper is part of a larger project aimed at looking into the formation and evolution of the Galactic disk by making use of a growing data base of photometric observations of as many OCs as possible. Thus, this study represents a further, intermediate step in a long-term programme devoted to obtain the fundamental parameters or to refine the quality of observationally determined properties for some unstudied or poorly studied OCs.

* E-mail: andres@iafe.uba.ar (AEP); claria@oac.uncor.edu (JJC); aahumada@eso.org (AVA)

$UBVI_{KC}$ photometry has proved to be a valuable tool to obtain the fundamental parameters of star clusters since information on cluster membership, distance, reddening, metallicity and age is obtained through the analysis of $(V, B - V)$ and $(V, V - I)$ Colour-Magnitude Diagrams (CMDs). In the year 2000, we carried out at Cerro Tololo Inter-American Observatory (CTIO, Chile) an observational program focused on still unstudied OCs at that time. We favoured the observation of OCs which were interesting not only because of the derivation of their basic parameters but also because of the possibility they offered of studying the morphology of their red giant evolutionary phases in relation to previous results (see, e.g., Mermilliod et al. 2001).

In this study, we report the results obtained from high-quality CCD $UBVI_{KC}$ photometry down to $V \approx 21.0$ in the fields of the selected OCs Berkeley 26, Czernik 27, Melotte 72, NGC 2479 and BH 37. These objects promised to be very interesting for their relatively old appearance due either to the observed stellar population in the CMDs or to their shapes and clustered nature. The basic parameters of the observed OCs are given in Table 1, where the Trumpler class was taken from Archinal & Hynes (2003). The last two columns list the total number of measured stars in this study and the inferred total number of cluster stars. The latter, together with the availability of a larger sample of data treated in the same way, will make it easier to establish a future calibration of the Trumpler richness class. All the selected clusters are located in the third Galactic quadrant near the Galactic plane ($|b| \leq 6^\circ$). A brief description of these OCs, along with earlier photometric observations, is given below.

Berkeley 26: Also known as Biurakan 12 (Iskudarian 1960) or C0647+058, this cluster seems to be a faint and probably old object in Monoceros. As indicated by its Trumpler class (III 1m), it shows no strong central concentration but can be identified by its relatively dense population compared to that of the field stars (Fig. 1). Using 2-Micron All-Sky Survey (2MASS) data, Tadross (2008) derived a heliocentric distance of 2.7 ± 0.1 kpc, $E(B - V) = 0.54$ and an age of 600 Myr. These values, however, do not agree at all with those recently obtained by Hasegawa, Sakamoto & Malasan (2008, hereafter HSM08) from CCD VI photometry carried out with a 65 cm telescope. In fact, according to these authors, Berkeley 26 is a very old (4.5 Gyr), highly reddened ($E(V - I) = 0.80$) and very distant ($d = 7.8$ kpc) OC.

Czernik 27: This is a relatively faint cluster first recognized in Monoceros by Czernik (1966). As indicated by its Trumpler class (III 1p), Czernik 27 (IAU designation C0700+064) is one of the most poorly defined objects of the present sample. It has a relatively small angular size of about $3'$ (Lyngå 1987). Kim et al. (2005) and HSM08 reported BV and VI CCD photometry in the cluster field, respectively. The cluster parameters determined in both cases, however, do not show a close correlation. Kim et al. (2005) found that Czernik 27 is a moderately reddened ($E(B - V) = 0.15$) Hyades like age cluster located at 5.8 kpc from the Sun, while HSM08 concluded that this is a slightly reddened ($E(B - V) \approx 0.08$) and older (1.1 Gyr) OC located at 4.3 kpc from the Sun.

Melotte 72: According to Archinal & Hynes (2003), this object is the same as Collinder 467 (Collinder 1931). They described it as a small, compressed cluster, with its core about $3'$ in diameter and with a $5'$ long stream extending to the north between the two bright stars HD 61277 ($V = 7.05$, K5) and HD 61401 ($V = 8.49$, B9). The cluster lies about 1.3° southwest of α Mon (Fig. 1). As far as we are aware, the only photometric study of this object was carried out by HSM08 using VI CCD images. They found this object to be an intermediate-age cluster (1.6 Gyr) located at a distance of 3.2 kpc, with reddening $E(V - I) = 0.10$.

NGC 2479: This object, also referred to as Collinder 167 (Collinder 1931), C0752-175 or Trumpler 8 (Trumpler 1930), is a relatively bright cluster in Puppis. As shown in Fig. 1, there are several bright stars in the cluster field, many of which seem to be foreground stars. Lyngå (1987) reported an angular diameter of $11'$ for NGC 2479. Kharchenko et al. (2005) presented a catalogue of astrophysical data for 520 Galactic OCs -among them NGC 2479- which could be identified in their All-Sky Compiled Catalogue (ASCC-2.5). By applying homogeneous methods and algorithms, they determined basic parameters for their cluster sample. For NGC 2479, they found the following results: $E(B - V) = 0.10$, $d = 1.2$ kpc and ~ 1 Gyr. We should be cautious, however, when considering these findings since the limiting magnitude of the ASCC-2.5 is $V \approx 12.5$.

BH 37: This is a detached, moderately rich and relatively faint OC (Fig. 1). As far as we know, no previous data exist for this compact object (IAU designation C0834-434) first recognized as an open cluster in Vela by van den Bergh & Hagen (1975).

The present photometric data are used to determine reddening, distance, age and metallicity of the selected OCs. The layout of the paper is as follows: Section 2 presents the observational material and the data reduction, whereas in Section 3 we determine the cluster centres and the stellar density radial profiles. In Section 4 we explain how to minimize the field star contamination in the CMDs. Section 5 deals with the determination of cluster fundamental parameters through the fitting of theoretical isochrones and with the comparison with previous results. Finally, Section 6 summarizes our findings and conclusions.

2 DATA COLLECTION AND REDUCTION

We obtained images for the cluster sample in December 2000 with the $UBVI_{KC}$ filters and a 2048×2048 pixel Tektronix CCD attached to the CTIO 0.9 m telescope. The detector used has a pixel size of $24 \mu\text{m}$, producing a scale on the chip of $0.4'' \text{pixel}^{-1}$ (focal ratio $f/13.5$) and a $13.6' \times 13.6'$ field of view. In order to standardize our photometry, we carried out observations of standard stars of the Selected Areas PG0231+051, 92 and 98 of Landolt (1992). By the end of each night, we had collected an average of 45 different measures of magnitude per filter for the selected standard star sample.

Table 2 shows the logbook of the observations with filters, exposure times, airmasses and seeing estimates. Observational setups, data reduction procedures, stellar point spread function photometry and transformation to the standard system, follow the same prescriptions described in detail in Piatti, Clariá & Ahumada (2009). The standard star photometry shows the mean square root deviation of the observations from the fits to be less than 0.015 mag, indicating that the nights were photometric. Once the standard magnitudes and colours were obtained, we produced a master table containing the average of V , $U - B$, $B - V$, and $V - I$, their errors $\sigma(V)$, $\sigma(U - B)$, $\sigma(B - V)$ and $\sigma(V - I)$ and the number of observations for each star, respectively. Tables 3 to 7 provide this information for Berkeley 26, Czernik 27, Melotte 72, NGC 2479 and BH 37, respectively. Only a portion of these tables is shown here for guidance regarding their form and content. Tables 3 to 7 are shown in entirety in the online version of the journal. The deepest CCD images obtained for the cluster sample are shown in Fig. 1. In most cases the cluster region is only a small part of the observed frame, as indicated by the solid circles.

A simple inspection of Tables 3 to 7 shows that stars with three measures of $B - V$ and $V - I$ colours extend from the brightest limit down to $V = 19$ mag and 20 mag, respectively. The stars with two measures of $B - V$ and $V - I$ colours cover V ranges from 13.0 to 20.0 mag and from 13.0 to 21 mag, respectively. Finally, the stars with only one measure of $B - V$ and $V - I$ are fainter than $V = 18.0$ and 19.0 mag, respectively, and they reach the photometric magnitude limits. According to these crude statistics, stars lying within the brightest ~ 6 mags of our ~ 9 mag range were measured two and three times. Therefore, they are the most appropriate ones to use to derive astrophysical information. The behaviour of the photometric errors for the V magnitude and $U - B$, $B - V$ and $V - I$ colours as a function of V is shown in Table 8. Since those observed only once have practically no statistical weight, we decided to use all the stars. In addition, the knowledge of the behaviour of the photometric errors with the magnitude for these stars, allows us to rely on the accuracy of the morphology and position of the main cluster features in the CMDs. The resulting CMDs are drawn in Figs. 3, 4 and 5 which show, in general, broad sequences. It should be noticed that since we have measured just a handful of stars in the U passband for Berkeley 26, we only show the $(V, B - V)$ and $(V, V - I)$ CMDs for this cluster.

Kim et al. (2005) obtained BV CCD photometry for stars in the field of Czernik 27. For 992 stars measured in common by Kim et al. (2005) and in this study, we derived $V_{\text{Kim}} - V_{\text{our}} = 0.35 \pm 0.07$ mag, $(B - V)_{\text{Kim}} - (B - V)_{\text{our}} = -0.05 \pm 0.11$ mag and $(V - I)_{\text{Kim}} - (V - I)_{\text{our}} = 0.07 \pm 0.08$ mag, with a marginal dependence with the magnitude (see Fig. 2). Since Kim et al. (2005) also found B and V magnitude offsets when comparing their photometry for Berkeley 29 with that of Kaluzny (1994), they decided to apply such offset to the Czernik 27's photometry. This prevented us from using their data as a photometric reference. Kim et al. (2005) also obtained BV data for only 18 stars in the field of NGC 2479 reaching a limiting magnitude of $V \approx 12.5$ -13.0 mag, so that only a small portion of the cluster Main Sequence (MS) could be traced. When comparing their magnitudes and colours with those observed by us, we find $V_{\text{k05}} - V_{\text{our}} = -0.03 \pm 0.39$ mag and $(B - V)_{\text{k05}} - (B - V)_{\text{our}} = -0.02 \pm 0.34$ mag. Recently, HSM08 published CCD VI photometry for Berkeley 26, Czernik 27 and Melotte 72. Unfortunately, since the data are neither available in the WEBDA database (Mermilliod & Paunzen 2003) nor upon request to the authors, we could not compare our photometry with theirs.

3 CLUSTER DIMENSIONS AND STRUCTURE

We first determined the location of the clusters' centres in order to construct stellar density profiles. The coordinates of the clusters' centres and their estimated uncertainties were determined, for each cluster, by fitting Gaussian distributions to the star counts in the x and y directions. The fits of the Gaussians were performed using the NGAUSSFIT routine in the STSDAS/IRAF package. We adopted a single Gaussian and fixed the constant to the corresponding background level and the linear terms to zero. The stars projected along the x and y directions were counted within intervals of 50 pixels. In addition, we checked that using spatial bins from 20 to 50 pixels or from 50 to 100 pixels does not lead to significant changes in the derived centres. We iterated the fitting procedure once on average, after eliminating a couple of discrepant points. Then, we determined the clusters' centres with a typical NGAUSSFIT standard deviation of ± 10 pixels. The centres of the Gaussians for Berkeley 26, Czernik 27, Melotte 72, NGC 2479 and BH 37 were finally fixed at $(x_c, y_c) = (1170, 1300)$, $(1320, 1270)$, $(1370, 1210)$, $(1215, 1250)$ and $(1230, 1030)$ pixels, respectively.

We constructed the clusters' radial profiles from star counts made in boxes of 50 pixels by 50 pixels, distributed throughout the whole field of each cluster. The chosen size of the box allowed us to sample, statistically, the stellar spatial distributions avoiding spurious effects caused mainly by the presence of localized groups of stars, rows or columns of stars. Thus, the number of stars per unit area, at a given radius r , can be directly calculated through the expression:

$$(n_{r+25} - n_{r-25}) / ((m_{r+25} - m_{r-25}) \times 50^2), \quad (1)$$

where n_j and m_j represent the number of stars and boxes included in a circle of radius j , respectively. Note that this method does not necessarily require a complete circle of radius r within the observed field to estimate the mean stellar density at such distance. This is important to consider since having a stellar density profile, which extends far away from the cluster centre, allows us to estimate the background level with higher precision. This is also helpful to measure the FWHM of the stellar density profile for it plays a significant role - from a stellar content point of view - in the construction of the cluster CMDs.

The resulting density profiles are shown in Fig. 6. The uncertainties estimated at various distances from the cluster centres follow Poisson statistics. Table 9 lists the estimated background levels, the radii at the FWHM (r_{FWHM}) and the field star contamination estimated in percentages. Note that the percentage of field stars is relatively high, which indicates a relatively small ratio between the number of each cluster's stars and the number of field stars. No cluster stands out clearly in its surrounding field within r_{FWHM} .

4 COLOUR MAGNITUDE DIAGRAM CLEANING

Without a careful analysis of the observed sequences in the CMDs, one could come to the conclusion that they are in fact the clusters' MSs. However, all the CMDs present both cluster and field star MSs more or less superimposed. This means that we have observed both star clusters and their respective foreground fields affected by nearly similar reddenings, which makes it difficult to separate the fiducial cluster features and renders the analysis of the CMDs challenging.

To statistically clean the cluster CMDs from stars that can potentially belong to the foreground/background fields, we built star field CMDs using the stars located in the easternmost strip of the observed fields, i.e., $x < 500$ pixels and $0 < y$ (pixels) < 2050 (see, Fig. 1). We separately treated the CMDs for $B - V$ and $V - I$. Using these field CMDs, we counted how many stars lie in different magnitude-colour bins with sizes $[\Delta V, \Delta(B - V) = \Delta(V - I)] = (0.5, 0.1)$ mag. We then subtracted from each cluster CMD the number of stars counted for each range of the field (V , $B - V$ or $V - I$) CMD, by removing those stars closer in magnitude and colour to the ones in the star field. Figs. 7, 8 and 9 show the CMDs of the cluster surrounding field regions, while Figs. 10, 11 and 12 show, with filled circles, the circular extracted CMDs which were obtained after cleaning them for field star contamination. We show overplotted the CMDs directly obtained with all the measured stars (dots). When comparing observed and cleaned cluster CMDs, the differences in stellar composition became evident. Although the fiducial features of some clusters looked clearer, they appeared somewhat dispersed and scattered. This is mainly due to some unavoidable field interference. Other sources of dispersion such as photometric errors, differential internal cluster reddening, evolutionary effects and binarity can also account for such effect. In the subsequent analysis, we used the cleaned CMDs to estimate the cluster fundamental parameters. Note that we will only use the extracted ($V, V - I$) CMD of Berkeley 26 since no star remains in its extracted ($V, B - V$) CMD.

5 ESTIMATES OF THE CLUSTERS FUNDAMENTAL PARAMETERS

In order to estimate the ages of the observed clusters, we used the Morphological Age Index (MAI) defined by Janes & Phelps (1994) on the basis of the δV , $\delta(B - V)1$ and $\delta(V - I)1$ indices of Phelps, Janes & Montgomery (1994) as well as the ΔV age index calibrated by Carraro & Chiosi (1994). We also illustrate possible solutions for the fundamental cluster parameters by matching theoretical isochrones computed by Lejeune & Schaerer (2001) to the observed CMDs. The previously known values of some cluster physical properties were used as reference to select the isochrones which best matched the CMDs.

Berkeley 26: the region delimited by $V < 18$ and $V - I > 1.4$ would seem to contain cluster giants. We derived an age between 2 and 6 Gyr from the ΔV index, which agrees with the age resulting from the MAI (2.0 - 5.5 Gyr). If we use a 4 Gyr isochrone, which corresponds to the average age obtained from the MAI and the ΔV index, and we match it to the observed ($V, V - I$) CMD, we then get a fit consistent with the data. Indeed, the theoretical turnoff and subgiant branch magnitudes, the loci of the MS and of the red giant branch (RGB), and the slope of the RGB, all appear to be reasonably located with respect to the observed features. Using isochrones of 2 or 6 Gyr, we did not find successful fits that reproduced the observed $V - I$ distance between the MS turnoff and the bluest RGB point.

Czernik 27: since it is not possible to obtain only one solution from the ZAMS fitting for the reddening-distance modulus pair, we assumed solar metallicity to evaluate which of both sets of published fundamental parameters (see Sect. 1) best resembles the fiducial features observed in the CMDs. We find the curvature and shape of the upper MS, the brightest magnitude of the MS and the bluest point of the turnoff, reasonably well fitted by the isochrones of 660 Myr and 1.1 Gyr.

Melotte 72: a Red Giant Clump (RGC) is visible at $V \sim 13$ mag and $B - V \sim V - I \sim 1.0$ mag. We derived an age between 0.4 and 1.0 Gyr from both the ΔV age index and the MAI. By using a solar metallicity 0.6 Gyr isochrone, it is possible to obtain a reasonable match to the cluster CMDs. The theoretical locus of the RGC, the brightest magnitude of the MS and the bluest point of the turnoff are the features which appear to be consistent with the data.

NGC 2479: the cluster shows a very long star sequence and a compact RGC at $V \sim 12$ and $U - B = V - I \sim 1.0$ mag. Firstly, we derived the colour excesses from both colour-colour diagrams, by shifting the ZAMS along the directions of the corresponding reddening vectors (Straizys 1992). Secondly, once the reddening effect was accounted for, we used the observed ZAMS ($V > 14$ mag) to obtain the apparent distance modulus. The cluster age turned out to be in the 0.6 - 1.2 Gyr range from both the MAI and the ΔV index. Moreover, by using a solar metallicity 1 Gyr isochrone, we achieved a good match to the fiducial features observed in the CMDs.

BH 37: the cluster CMDs present a possible red giant branch and a reasonably well-defined evolved upper MS, particularly in the $(V, V - I)$ CMD. As the cluster has not been studied in detail yet, we attempted a subjective isochrone match to the cluster CMDs.

Schlegel, Finkbeiner & Davis's (1998, hereafter SFD) obtained full-sky maps from 100-m dust emission. They found that in high Galactic latitude regions, the dust map correlates well with maps of HI emission. However, deviations are coherent in the sky and are especially conspicuous in regions of HI emission saturation towards denser clouds and in regions of formation of H_2 in molecular clouds (Piatti et al. 2003; Piatti et al. 2008). Even if the SFD's reddenings would not be exactly correct, they may still be valuable to compare with the reddenings derived here. We obtained $E(B - V)_{SFD}$ values of 0.61, 0.19, 0.22, 0.16 and 2.19 mags for Berkeley 26, Czernik 27, Melotte 72, NGC 2479 and BH 37, respectively. Since the $E(B - V)_{SFD}$ value for BH 37 turned out to be more than double the one we estimated, we assumed that the $E(B - V)_{SFD}$ value must be saturated. It is worth considering that the ve clusters lie further than 70 pc from the Galactic plane, with heights out of the Galactic plane of 0.17 kpc, 0.49 kpc, 0.28 kpc, 0.14 kpc and -0.07, respectively.

Table 10 shows the values of the resulting fundamental parameters, while Figs. 13, 14 and 15 indicate how the isochrones match the cluster features in the CMDs. Note that these values illustrate only possible solutions for the cluster fundamental parameters. Such solutions prove to be consistent with the data obtained. Fig. 13 shows that the MS of Berkeley 26 is very broad, probably due to differential reddening and field star contamination. Although the three brighter and bluer stars than the turnoff are considered to be foreground stars, some of them could be blue stragglers. Similarly, some of the brighter and bluer stars than the MS turnoff of Czernik 27 (Fig. 14) should also be considered blue straggler candidates. In order to improve the trace of the cluster features, it would be of great value to carry out deeper MS photometry and spectroscopic observations of the red giant branch. Note that the theoretically computed bluest stage, during the core He-burning phase, is redder than the observed RGC in the CMDs of Melotte 72, a behaviour which has also been detected in other studies of Galactic and Magellanic Cloud clusters (Geisler et al. 2003; Piatti, Clariá & Ahumada 2004a; Piatti, Clariá & Ahumada 2004b, for example).

5.1 Comparison with previous results

Berkeley 26 : The cluster parameters found here are very different from those found by Tadross (2008) from archival *JHK* 2MASS photometry. By inspecting the CMDs obtained by Tadross to derive the cluster parameters (see his Fig. 6), we realized that he did not include upper MS and red giant branch stars. This error could have been due to the methods he employed for cleaning the CMDs and for selecting the cluster stars. In addition, the isochrone fit to the cluster CMDs does not resemble the cluster sequence at all. Our findings show a better agreement with the parameters recently determined by HSM08 from *VI* CCD photometry. In fact, in their study and in ours, the old and metal-poor character of Berkeley 26 is confirmed. Although the reddening derived in both studies agrees, within the errors, the heliocentric distance found by HSM08 is larger than ours.

Czernik 27 : Using Girardi et al.'s (2002) isochrones for solar metallicity content, Kim et al. (2005) estimated a cluster $E(B - V)$ reddening of 0.15, a distance from the Sun of 5.8 kpc, and an age of 600 Myr. HSM08 recently reported *VI* CCD photometry in the cluster field. The parameters they found, however, do not show agreement, in general terms, with those derived by Kim et al. (2005). Actually, according to HSM08, Czernik 27 seems to be reddened by scarcely $E(V - I) = 0.10$, it is located closer to the Sun (4.3 kpc) and it is about 1.1 Gyr old. However, we find that both sets of parameters reasonably reproduce the current CMDs we obtained for the cluster (see Fig. 14).

Melotte 72 : As far as we are aware, the only detailed study of this cluster was carried out by HSM08. Their heliocentric distance and metallicity are similar with our adopted values, their reddening ($E(V - I) = 0.25$) and age (= 1.6 Gyr) being somewhat larger. However, when comparing their $(V, V - I)$ CMD for the central part of the cluster (see their Fig. 2) with our $(V, V - I)$ CMD (Fig. 14), we see that the turnoff of their selected isochrone is fainter than the turnoff we observed. We believe that the fit would have been much better if they had used a younger isochrone.

NGC 2479 : The catalogue by Kharchenko et al. (2005), based on the information provided by their ASCC-2.5, includes an analysis of 20 stars in the cluster field with B, V magnitudes and proper motions in the Hipparcos system. Only a small portion of the cluster MS can be traced due to the limiting magnitude of these stars, which reaches $V \approx 12.5$ -13.0 mag. Based on a comprehensive analysis to determine membership, Kharchenko et al. showed that the 20 stars should be members according to the photometric data they used, although only four of them have proper motion membership probabilities higher than 80%. The 20 stars do not define any clear MS in the $(V, B - V)$ CMD, while the four stars with the highest proper motion membership probabilities are located between the cluster turnoff and the RGC. For comparison purposes, we have

drawn these stars with open circles in Fig. 15. Surprisingly, all the cluster parameters determined by Kharchenko et al. (i.e., distance, age, reddening, core and cluster radii, etc.) coincide with our estimates.

6 SUMMARY AND CONCLUSIONS

New CCD $UBVI_{KC}$ photometry in the field of the open clusters Berkeley 26, Czernik 27, Melotte 72, NGC 2479 and BH 37 is reported here. The analysis of the photometric data leads to the following main conclusions:

(i) Once the cluster centres were determined by fitting Gaussian distributions to the star counts in the x and y directions, radial density profiles were produced.

(ii) Cluster CMDs cleaned from field star contamination were built by statistically subtracting the number of stars counted in the field CMDs. Those stars closer in magnitude and colour to the ones in the respective star fields were thus removed.

(iii) Estimates of the cluster ages were obtained for Berkeley 26, Melotte 72 and NGC 2479 from both the ΔV age index and the MAI. On the other hand, we outlined possible solutions for cluster fundamental parameters by matching theoretical isochrones, which reasonably reproduce the main cluster features in their CMDs. In the case of NGC 2479, the $E(B - V)$ and $E(V - I)$ colour excesses and apparent distance modulus were estimated from the fit of the ZAMS to the colour-colour and magnitude-colour diagrams, respectively.

ACKNOWLEDGEMENTS

We are gratefully indebted to the CTIO staff for their hospitality and support during the observations. We also thank referees Bruce Twarog and Kenneth Janes whose comments and suggestions have helped us to improve the manuscript. This work was partially supported by the Argentinian institutions CONICET, SECYT (Universidad Nacional de Córdoba) and Agencia Nacional de Promoción Científica y Tecnológica (ANPCyT). This work is based on observations made at Cerro Tololo Inter-American Observatory, which is operated by AURA, Inc., under cooperative agreement with the National Science Foundation. This research also used the SIMBAD database, operated at CDS, Strasbourg, France; also the WEBDA database, operated at the Institute for Astronomy of the University of Vienna, and the NASA's Astrophysics Data.

REFERENCES

- Archinal B.A., Hynes S.J. 2003, *Star Clusters*, Willman-Bell, Richmond VA
- Carraro G., Chiosi C. 1994, *A&A*, 287, 761
- Chen L., Hou J.L., Wang J.J., 2003, *AJ*, 125, 1397
- Collinder p., 1931, *Medd. Lunds Astron. Observatorium* 2
- Czernik M. 1966, *Acta Astron.*, 16, 93
- Dean F.J., Warren P.R., Cousins A.W.J. 1978, *MNRAS*, 183, 569
- Friel E.D. 1995, *ARA&A*, 33, 81
- Geisler D., Piatti A.E., Bica E., Clariá J.J. 2003, *MNRAS*, 341, 771
- Girardi L., Bertelli G., Bressan A., Chiosi C., Groenewegen M.A.T., et al. 2002, *A&A*, 391, 195
- Hasegawa T., Sakamoto T., Malasan H.L. 2008, *Publ. Astron. Soc. Japan* 60, 1267 (HSM08)
- Iskudarian S.G. 1960, *Soobshch Byurakan Obs.* 28, 43
- Janes K.A., Adler D., 1982, *ApJS*, 49, 425
- Janes K.A., Phelps R.L., 1994, *AJ*, 108, 1773
- Kaluzny J. 1994, *A&AS*, 108, 151
- Kharchenko N.V., Piskunov A.E., Röser, S., Schilbach E., Scholz R.-D. 2005, *A&A*, 438, 1163
- Kim S.C., Park H.S., Sohn S.T., Lee M.G., Park B.-G., Sung H., Ann H.B., Chun M.-Y., Kim S.-L., Jeon Y.-B., Yuk I.-S., Lee S.H. 2005, *Journal of The Korean Astronomical Society*, 38, 1
- Landolt A. 1992 *AJ*, 104, 340
- Lejeune T., Schaerer D. 2001, *A&A*, 366, 538
- Lyngå G. 1987, *Catalogue of Open Cluster Data*, Centre de Données Stellaires, Strasbourg
- Mermilliod J.-C., Clariá J.J., Andersen J., Piatti A.E., Mayor M. 2001, *A&A*, 375, 30
- Mermilliod, J.-C., & Paunzen, E. 2003, *WEBDA Open Cluster Database*, *A&A*, 410, 511
- Meynet G., Mermilliod J.-C., Maeder A., 1993, *A&AS*, 98, 477
- Phelps R., Janes K., Montgomery K.A. 1994, *AJ*, 107, 1079
- Piatti A.E., Clariá J.J., Ahumada A.V. 2004a, *A&A*, 418, 979
- Piatti A.E., Clariá J.J., Ahumada A.V. 2004b, *A&A*, 421, 991
- Piatti A.E., Clariá J.J., Ahumada A.V. 2009, *MNRAS*, 397, 1073
- Piatti A.E., Geisler D., Bica E., Clariá J.J. 2003, *MNRAS*, 343, 851
- Piatti A.E., Geisler D., Sarajedini A., Gallart C., Wischnjewsky M. 2008, *MNRAS*, 389, 429
- Sandage A.R., 1988, in Philip A.G.D. Davis L., eds, *Calibration of Stellar ages*, Schenectady, USA, p. 43
- Schlegel D.J., Finkbeiner D.P., Davis M. 1998, *ApJ*, 500, 525 (SFD)

- Straizys V 1992, *Multicolor Stellar Photometry*, Pachart Publishing House, Tucson, Arizona
Tadross A.L. 2008, MNRAS, 389, 285
Trumpler R.J. 1930, Lick Obs. Bull., 14, 154
Twarog B.A., Ashman K.M., Anthony-Twarog B.J. 1997, AJ, 114, 2556
van den Bergh S., Hagen G.L. 1975, AJ, 80, 11

Table 1. Basic parameters of the five open clusters.

| Cluster | α_{2000} (h m s) | δ_{2000} ($^{\circ}$ ' ") | l ($^{\circ}$) | b ($^{\circ}$) | Trumpler Class | Angular Diameter (') | Number of measured stars | Number of inferred cluster stars |
|-------------|----------------------------|--------------------------------------|-----------------------|-----------------------|----------------|-------------------------|-----------------------------|-------------------------------------|
| Berkeley 26 | 6 50 18 | 5 45 00 | 207.69 | 2.35 | III 1m | 4.0 | 2226 | 97 |
| Czernik 27 | 7 03 22 | 6 23 47 | 208.58 | 5.56 | III 1p | 3.0 | 2385 | 188 |
| Melotte 72 | 7 38 24 | -10 41 00 | 227.84 | 5.36 | III 1m | 5.0 | 2770 | 107 |
| NGC 2479 | 7 55 04 | -17 42 35 | 235.98 | 5.37 | III 1m | 11.0 | 2490 | 38 |
| BH 37 | 8 35 49 | -43 37 00 | 262.35 | -1.78 | II 1m | 3.0 | 3000 | 65 |

Table 2. Observations log of selected clusters.

| Cluster | date | filter | exposure (sec) | airmass | seeing (") |
|-------------|---------------|----------|-------------------|---------|---------------|
| Berkeley 26 | Dec. 29, 2000 | <i>U</i> | 60 | 1.24 | 1.5 |
| | | <i>U</i> | 420 | 1.24 | 1.4 |
| | | <i>V</i> | 20 | 1.24 | 1.2 |
| | | <i>V</i> | 60 | 1.24 | 1.4 |
| | | <i>V</i> | 200 | 1.23 | 1.4 |
| | | <i>I</i> | 10 | 1.23 | 1.1 |
| | | <i>I</i> | 90 | 1.23 | 1.4 |
| Czernik 27 | Dec. 23, 2000 | <i>I</i> | 90 | 1.24 | 1.2 |
| | | <i>B</i> | 20 | 1.30 | 1.8 |
| | | <i>B</i> | 60 | 1.30 | 2.0 |
| | | <i>B</i> | 360 | 1.30 | 2.0 |
| | | <i>V</i> | 20 | 1.32 | 1.6 |
| | | <i>V</i> | 60 | 1.32 | 2.0 |
| | | <i>V</i> | 200 | 1.32 | 2.0 |
| Melotte 72 | Dec. 24, 2000 | <i>I</i> | 10 | 1.28 | 1.1 |
| | | <i>I</i> | 90 | 1.28 | 1.3 |
| | | <i>B</i> | 20 | 1.08 | 1.8 |
| | | <i>B</i> | 60 | 1.08 | 1.9 |
| | | <i>B</i> | 360 | 1.08 | 1.9 |
| | | <i>V</i> | 20 | 1.09 | 1.3 |
| | | <i>V</i> | 60 | 1.09 | 1.6 |
| NGC 2479 | Dec. 29, 2000 | <i>V</i> | 360 | 1.08 | 1.6 |
| | | <i>I</i> | 10 | 1.07 | 1.3 |
| | | <i>I</i> | 90 | 1.07 | 1.3 |
| | | <i>U</i> | 20 | 1.30 | 1.8 |
| | | <i>U</i> | 540 | 1.04 | 1.5 |
| | | <i>B</i> | 20 | 1.03 | 1.6 |
| | | <i>B</i> | 60 | 1.03 | 1.6 |
| BH 37 | Dec. 24, 2000 | <i>B</i> | 360 | 1.03 | 1.5 |
| | | <i>V</i> | 20 | 1.02 | 2.0 |
| | | <i>V</i> | 60 | 1.02 | 1.4 |
| | | <i>V</i> | 200 | 1.03 | 1.3 |
| | | <i>I</i> | 10 | 1.02 | 1.1 |
| | | <i>I</i> | 90 | 1.02 | 1.3 |
| | | <i>I</i> | 90 | 1.02 | 1.3 |
| BH 37 | Dec. 24, 2000 | <i>B</i> | 20 | 1.03 | 1.3 |
| | | <i>B</i> | 60 | 1.03 | 1.4 |
| | | <i>B</i> | 360 | 1.03 | 1.5 |
| | | <i>V</i> | 20 | 1.03 | 1.3 |
| | | <i>V</i> | 60 | 1.03 | 1.4 |
| | | <i>V</i> | 360 | 1.03 | 1.4 |
| | | <i>I</i> | 10 | 1.03 | 1.2 |
| <i>I</i> | 90 | 1.03 | 1.3 | | |

Table 3. CCD VI data of stars in the field of Berkeley 26.

| ID | x (pix) | y (pix) | V (mag) | $\sigma(V)$ (mag) | n_V | $V - I$ (mag) | $\sigma(V - I)$ (mag) | n_{VI} |
|-----|--------------|--------------|--------------|----------------------|-------|------------------|--------------------------|----------|
| ... | ... | ... | ... | ... | . | ... | ... | . |
| 70 | 1400.643 | 61.032 | 19.420 | 0.067 | 1 | 1.345 | 0.084 | 1 |
| 71 | 1122.117 | 61.227 | 18.361 | 0.031 | 3 | 1.565 | 0.072 | 2 |
| 72 | 1370.823 | 62.633 | 18.533 | 0.053 | 2 | 1.332 | 0.004 | 2 |
| ... | ... | ... | ... | ... | . | ... | ... | . |
| ... | ... | ... | ... | ... | . | ... | ... | . |
| ... | ... | ... | ... | ... | . | ... | ... | . |

NOTE: (x,y) coordinates correspond to the reference system of Fig. 1. Magnitude and colour errors are the standard deviations of the mean or the observed photometric errors for stars with only one measurement.

Table 4. CCD BVI data of stars in the field of Czernik 27.

| ID | x (pix) | y (pix) | V (mag) | $\sigma(V)$ (mag) | n_V | $B - V$ (mag) | $\sigma(B - V)$ (mag) | n_{BV} | $V - I$ (mag) | $\sigma(V - I)$ (mag) | n_{VI} |
|-----|--------------|--------------|--------------|----------------------|-------|------------------|--------------------------|----------|------------------|--------------------------|----------|
| ... | ... | ... | ... | ... | . | ... | ... | . | ... | ... | . |
| 88 | 399.518 | 68.806 | 15.750 | 0.044 | 3 | 0.714 | 0.027 | 2 | 0.816 | 0.067 | 3 |
| 89 | 419.049 | 70.068 | 16.170 | 0.062 | 3 | 0.643 | 0.029 | 2 | 0.745 | 0.073 | 3 |
| 90 | 1737.327 | 71.037 | 20.173 | 0.049 | 1 | 99.999 | 9.999 | 0 | 1.255 | 0.095 | 1 |
| ... | ... | ... | ... | ... | . | ... | ... | . | ... | ... | . |
| ... | ... | ... | ... | ... | . | ... | ... | . | ... | ... | . |
| ... | ... | ... | ... | ... | . | ... | ... | . | ... | ... | . |

NOTE: (x,y) coordinates correspond to the reference system of Fig. 1. Magnitude and colour errors are the standard deviations of the mean or the observed photometric errors for stars with only one measurement.

Table 5. CCD BVI data of stars in the field of Melotte 72.

| ID | x (pix) | y (pix) | V (mag) | $\sigma(V)$ (mag) | n_V | $B - V$ (mag) | $\sigma(B - V)$ (mag) | n_{BV} | $V - I$ (mag) | $\sigma(V - I)$ (mag) | n_{VI} |
|-----|--------------|--------------|--------------|----------------------|-------|------------------|--------------------------|----------|------------------|--------------------------|----------|
| ... | ... | ... | ... | ... | . | ... | ... | . | ... | ... | . |
| 402 | 1684.695 | 300.844 | 20.853 | 0.145 | 2 | 1.727 | 0.195 | 1 | 1.831 | 0.144 | 2 |
| 403 | 1751.192 | 302.558 | 20.173 | 0.033 | 2 | 1.152 | 0.066 | 1 | 1.257 | 0.032 | 2 |
| 404 | 1759.010 | 304.554 | 19.237 | 0.001 | 3 | 0.891 | 0.012 | 2 | 0.995 | 0.024 | 3 |
| ... | ... | ... | ... | ... | . | ... | ... | . | ... | ... | . |
| ... | ... | ... | ... | ... | . | ... | ... | . | ... | ... | . |
| ... | ... | ... | ... | ... | . | ... | ... | . | ... | ... | . |

NOTE: (x,y) coordinates correspond to the reference system of Fig. 1. Magnitude and colour errors are the standard deviations of the mean or the observed photometric errors for stars with only one measurement.

Table 6. CCD $UBVI$ data of stars in the field of NGC 2479.

| ID | x (pix) | y (pix) | V (mag) | $\sigma(V)$ (mag) | n_V | $U - B$ (mag) | $\sigma(U - B)$ (mag) | n_{UB} | $B - V$ (mag) | $\sigma(B - V)$ (mag) | n_{BV} | $V - I$ (mag) | $\sigma(V - I)$ (mag) | n_{VI} |
|-----|--------------|--------------|--------------|----------------------|-------|------------------|--------------------------|----------|------------------|--------------------------|----------|------------------|--------------------------|----------|
| ... | ... | ... | ... | ... | . | ... | ... | . | ... | ... | . | ... | ... | . |
| 11 | 988.318 | 390.190 | 18.199 | 0.010 | 3 | 1.414 | 0.106 | 1 | 0.849 | 0.022 | 1 | 1.335 | 0.009 | 3 |
| 12 | 1700.800 | 1030.361 | 18.505 | 0.024 | 3 | 0.674 | 0.014 | 2 | 0.645 | 0.003 | 2 | 0.990 | 0.023 | 3 |
| 13 | 158.117 | 1768.943 | 16.464 | 0.011 | 3 | 0.105 | 0.002 | 2 | 0.446 | 0.007 | 3 | 0.658 | 0.011 | 3 |
| ... | ... | ... | ... | ... | . | ... | ... | . | ... | ... | . | ... | ... | . |
| ... | ... | ... | ... | ... | . | ... | ... | . | ... | ... | . | ... | ... | . |
| ... | ... | ... | ... | ... | . | ... | ... | . | ... | ... | . | ... | ... | . |

NOTE: (x,y) coordinates correspond to the reference system of Fig. 2. Magnitude and colour errors are the standard deviations of the mean or the observed photometric errors for stars with only one measurement.

Table 7. CCD *BVI* data of stars in the field of BH 37.

| ID | x (pix) | y (pix) | V (mag) | $\sigma(V)$ (mag) | n_V | $B - V$ (mag) | $\sigma(B - V)$ (mag) | n_{BV} | $V - I$ (mag) | $\sigma(V - I)$ (mag) | n_{VI} |
|-----|--------------|--------------|--------------|----------------------|-------|------------------|--------------------------|----------|------------------|--------------------------|----------|
| ... | ... | ... | ... | ... | . | ... | ... | . | ... | ... | . |
| 142 | 1227.468 | 100.013 | 17.589 | 0.028 | 2 | 1.250 | 0.036 | 2 | 1.523 | 0.039 | 2 |
| 143 | 1455.322 | 100.024 | 19.965 | 0.011 | 2 | 1.374 | 0.080 | 1 | 1.646 | 0.125 | 2 |
| 144 | 1476.955 | 100.562 | 21.489 | 0.098 | 1 | 99.999 | 9.999 | 0 | 2.185 | 0.131 | 1 |
| ... | ... | ... | ... | ... | . | ... | ... | . | ... | ... | . |
| ... | ... | ... | ... | ... | . | ... | ... | . | ... | ... | . |
| ... | ... | ... | ... | ... | . | ... | ... | . | ... | ... | . |

NOTE: (x, y) coordinates correspond to the reference system of Fig. 1. Magnitude and colour errors are the standard deviations of the mean or the observed photometric errors for stars with only one measurement.

Table 8. Magnitude and colour photometric errors as a function of V .

| ΔV (mag) | $\sigma(V)$ (mag) | $\sigma(U - B)$ (mag) | $\sigma(B - V)$ (mag) | $\sigma(V - I)$ (mag) |
|---------------------|----------------------|--------------------------|--------------------------|--------------------------|
| 11-12 | < 0.01 | 0.01 | < 0.01 | < 0.01 |
| 12-13 | < 0.01 | 0.02 | 0.01 | 0.01 |
| 13-14 | < 0.01 | 0.02 | 0.01 | 0.01 |
| 14-15 | 0.01 | 0.03 | 0.01 | 0.02 |
| 15-16 | 0.01 | 0.04 | 0.01 | 0.02 |
| 16-17 | 0.02 | 0.04 | 0.02 | 0.02 |
| 17-18 | 0.02 | 0.05 | 0.02 | 0.03 |
| 18-19 | 0.03 | 0.06 | 0.03 | 0.03 |
| 19-20 | 0.03 | 0.07 | 0.05 | 0.05 |
| 20-21 | 0.05 | 0.10 | 0.10 | 0.10 |
| 21-22 | 0.10 | — | — | 0.15 |

Table 9. Cluster sizes and field contamination.

| Name | Background ^a (counts) | r_{FWHM} (px) | Field contamination (%) $r < r_{FWHM}$ |
|-------------|-------------------------------------|--------------------|---|
| Berkeley 26 | 3.6 | 140 ± 15 | 19 |
| Czernik 27 | 4.3 | 125 ± 15 | 41 |
| Melotte 72 | 5.0 | 200 ± 15 | 57 |
| NGC 2479 | 5.0 | 150 ± 15 | 63 |
| BH 37 | 5.0 | 180 ± 15 | 43 |

^a Normalized to a circular area of radius 50 pixels.

Table 10. Possible solutions for the fundamental parameters of the selected clusters.

| | Berkeley 26 | Czernik 27 | Melotte 72 | NGC 2479 | BH 37 |
|------------------|-------------|-------------|------------|----------|-------|
| $E(B - V)$ (mag) | 0.75 | 0.08 / 0.15 | 0.20 | 0.05 | 1.05 |
| $E(V - I)$ (mag) | 0.95 | 0.10 / 0.20 | 0.25 | 0.07 | 1.30 |
| $m - M_V$ (mag) | 15.50 | 13.4 / 14.3 | 13.00 | 11.00 | 15.25 |
| Age (Gyr) | 4 | 0.7 / 1.1 | 0.60 | 1.00 | 0.70 |
| [Fe/H] (dex) | -0.7 | 0.0 | 0.0 | 0.0 | 0.0 |

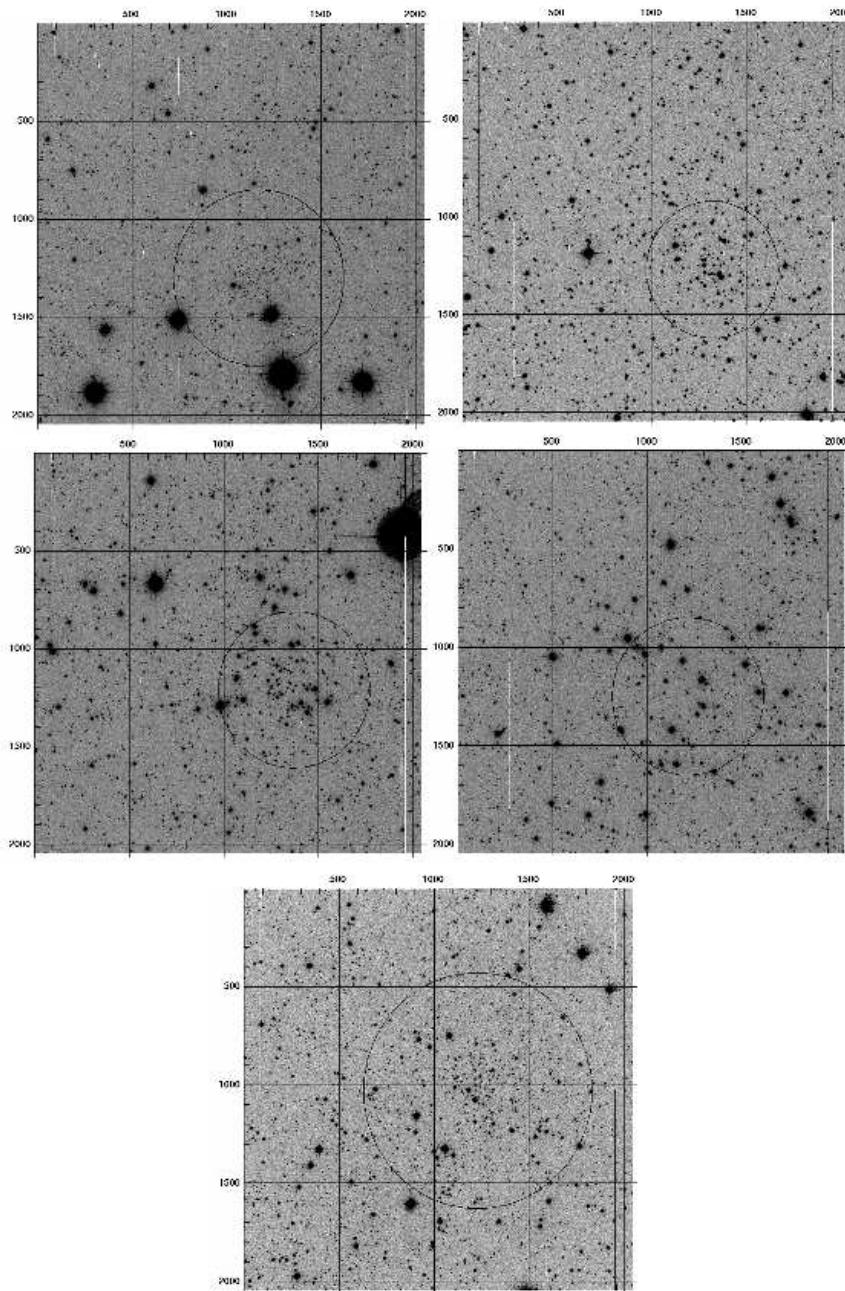


Figure 1. Deepest CCD images obtained : 90 s *I* for Berkeley 26 (*top left*); 360 s *B* for Czernik 27 (*top right*); 90 s *I* for Melotte 72

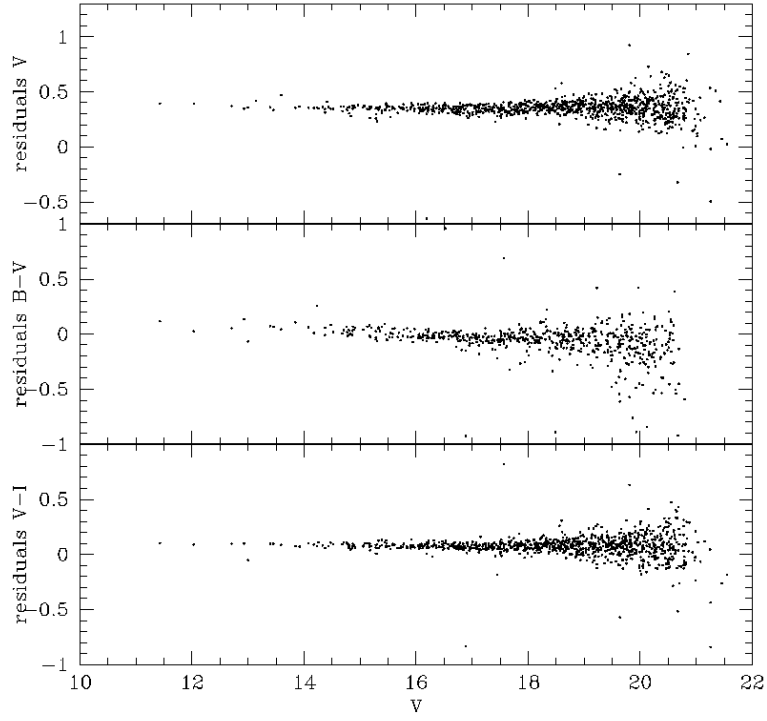


Figure 2. Comparison between our photometry for Czernik 27 and that of Kim et al. (2005).

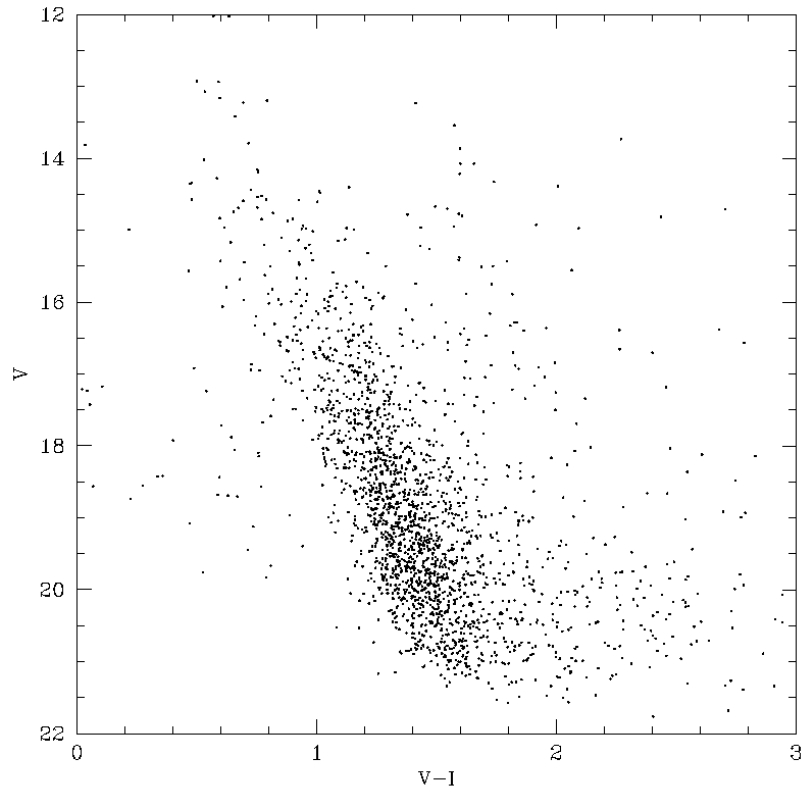


Figure 3. The $(V, V - I)$ diagram for the stars measured in the field of Berkeley 26.

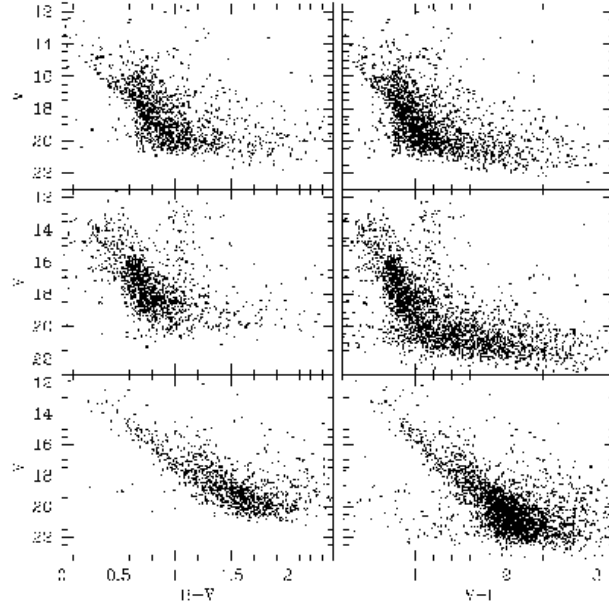


Figure 4. The $(V, B - V)$ and $(V, V - I)$ diagrams for the stars measured in the fields of Czernik 27 (*top*), Melotte 72 (*middle*) and BH 37 (*bottom*).

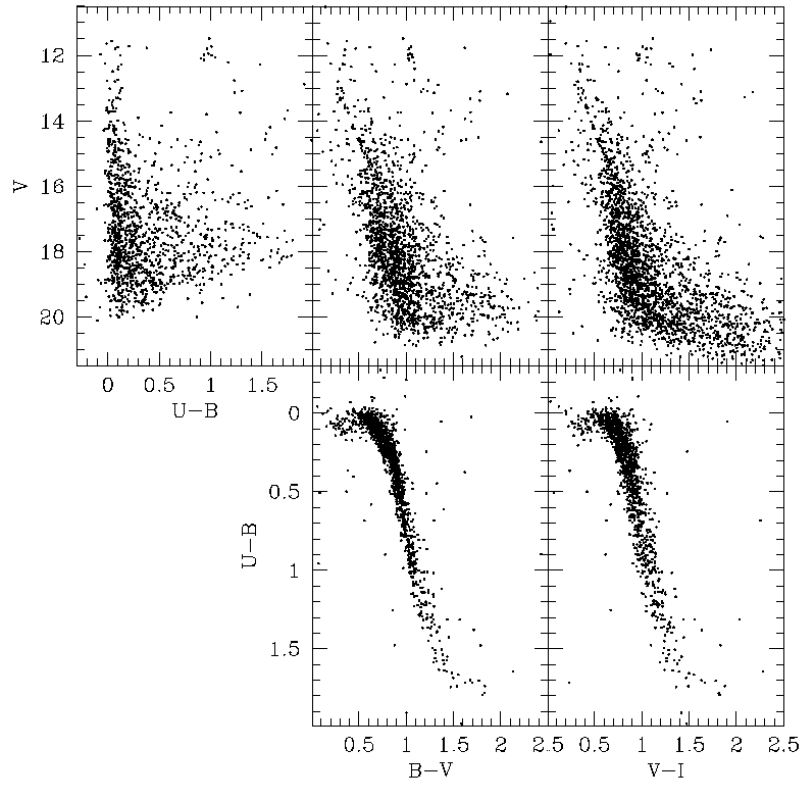


Figure 5. The $(V, U - B)$, $(V, B - V)$, and $(V, V - I)$ diagrams (*top*), and $(U - B, B - V)$ and $(B - V, V - I)$ diagrams (*bottom*) for the stars measured in the field of NGC 2479.

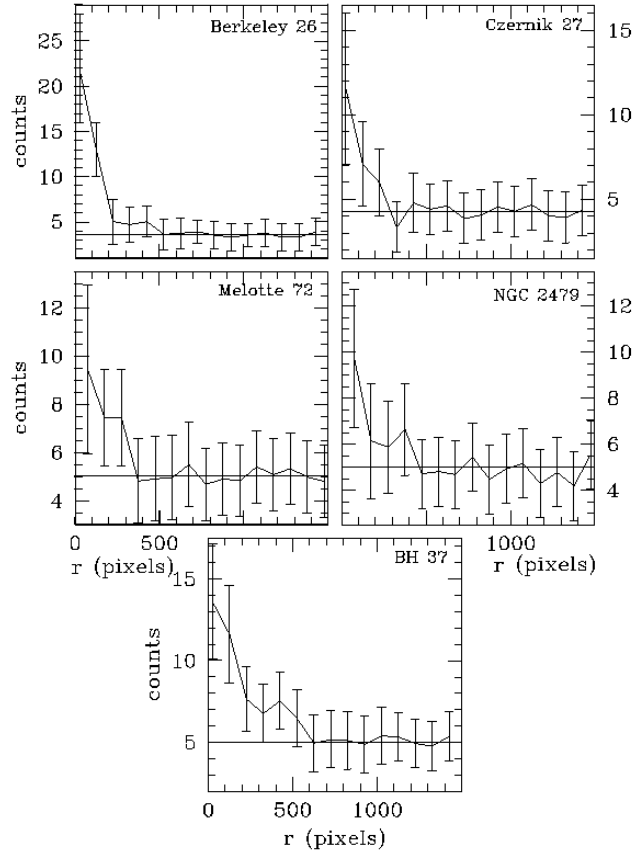


Figure 6. Cluster stellar density radial profiles normalized to a circular area of 50 pixel radius. The horizontal lines represent the measured background levels (see Section 3 for details).

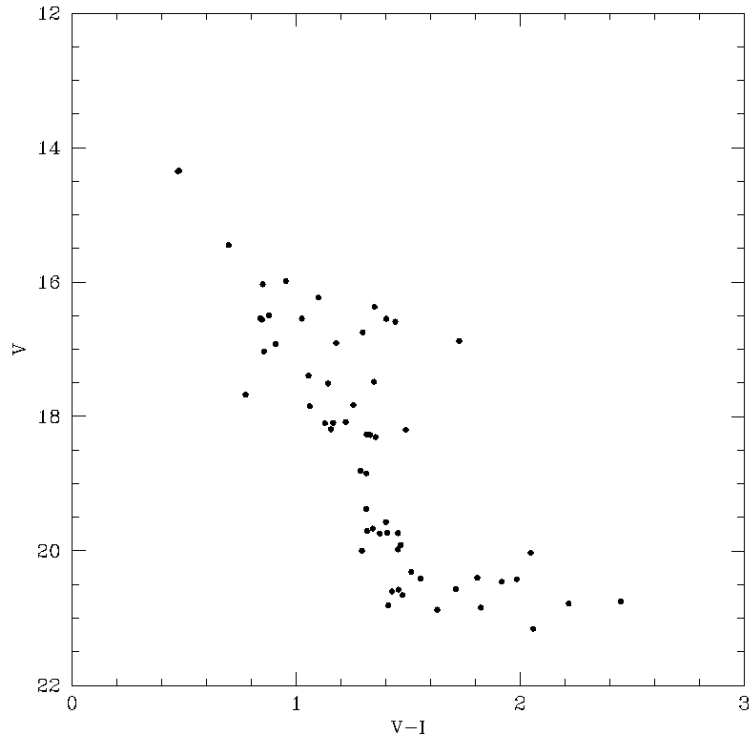


Figure 7. The $(V, V - I)$ diagram for the surrounding field region of Berkeley 26, normalized to a circular area of radius 200 pixels for comparison with Fig. 10.

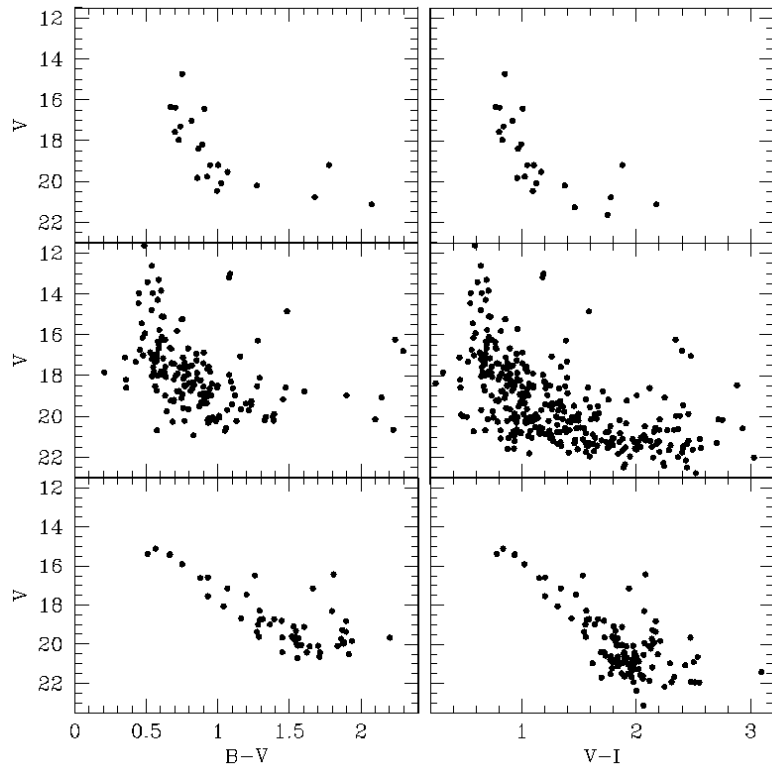


Figure 8. The $(V, B - V)$ and $(V, V - I)$ diagrams for the surrounding field regions of Czernik 27 (*top*), Melotte 72 (*middle*) and BH 37 (*bottom*), normalized to a circular area of radius 200 pixels for comparison with Fig. 11.

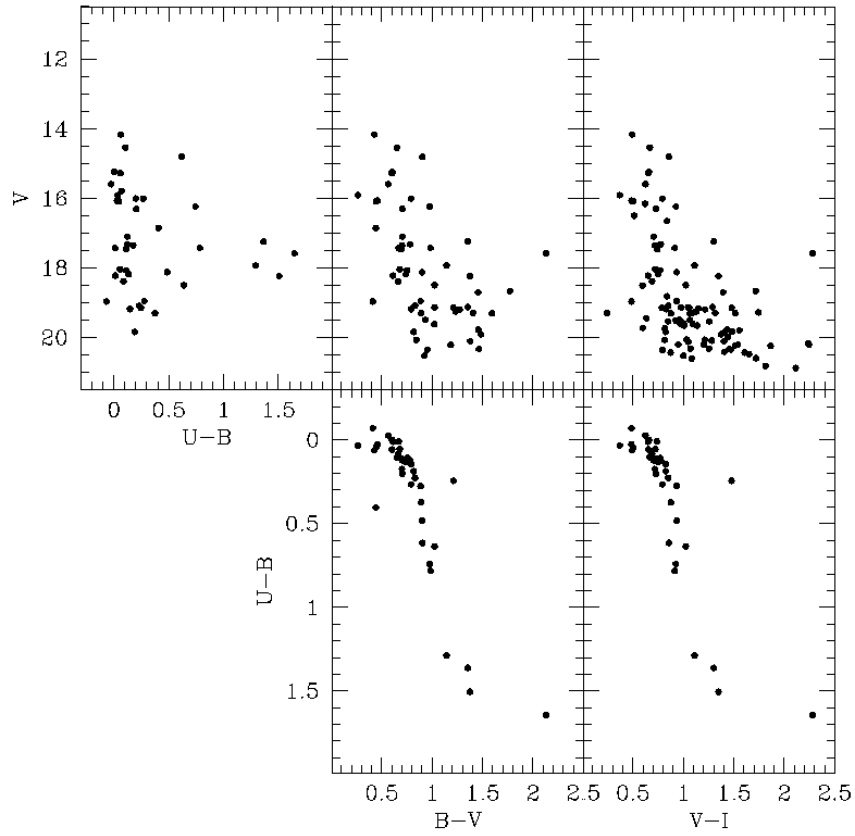


Figure 9. The $(V, U - B)$, $(V, B - V)$, and $(V, V - I)$ diagrams (*top*), and $(U - B, B - V)$ and $(B - V, V - I)$ diagrams (*bottom*) for the surrounding field region of NGC 2479, normalized to a circular area of radius 200 pixels for comparison with Fig. 12.

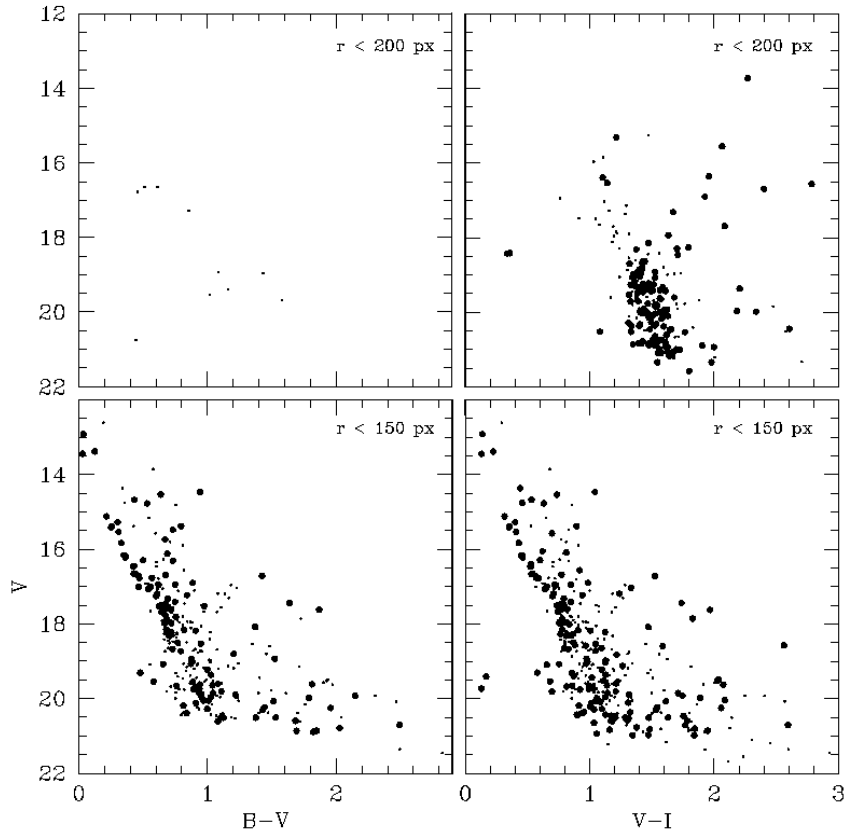


Figure 10. The circular extracted ($V, B - V$) and ($V, V - I$) diagrams for the clusters (dots) Berkeley 26 (*top*) and Czernik 27 (*bottom*), compared with those statistically cleaned from field star contamination (filled circles).

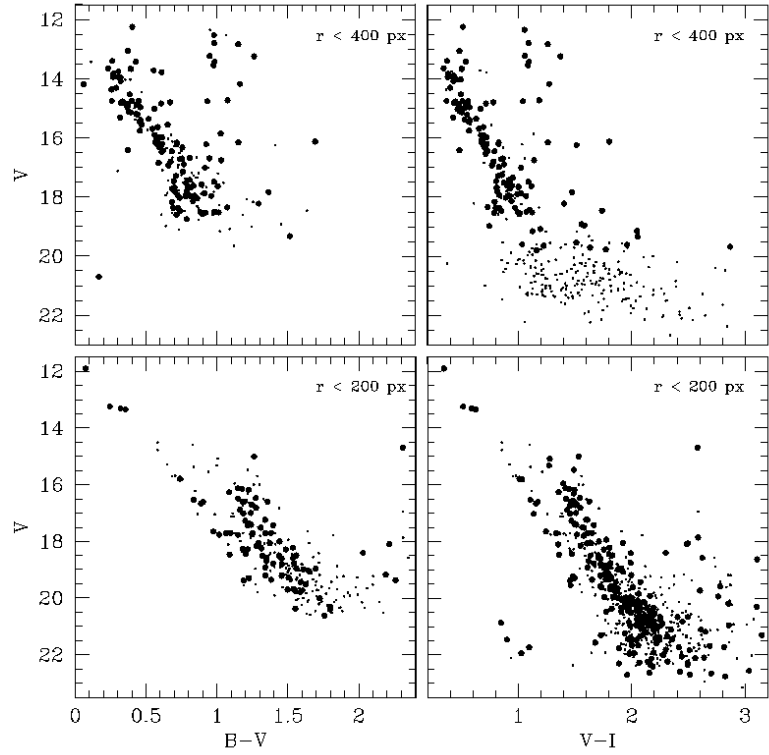


Figure 11. The circular extracted $(V, B - V)$ and $(V, V - I)$ diagrams for the clusters (dots) Melotte 72 (*top*) and BH 37 (*bottom*), compared with those statistically cleaned from field star contamination (filled circles).

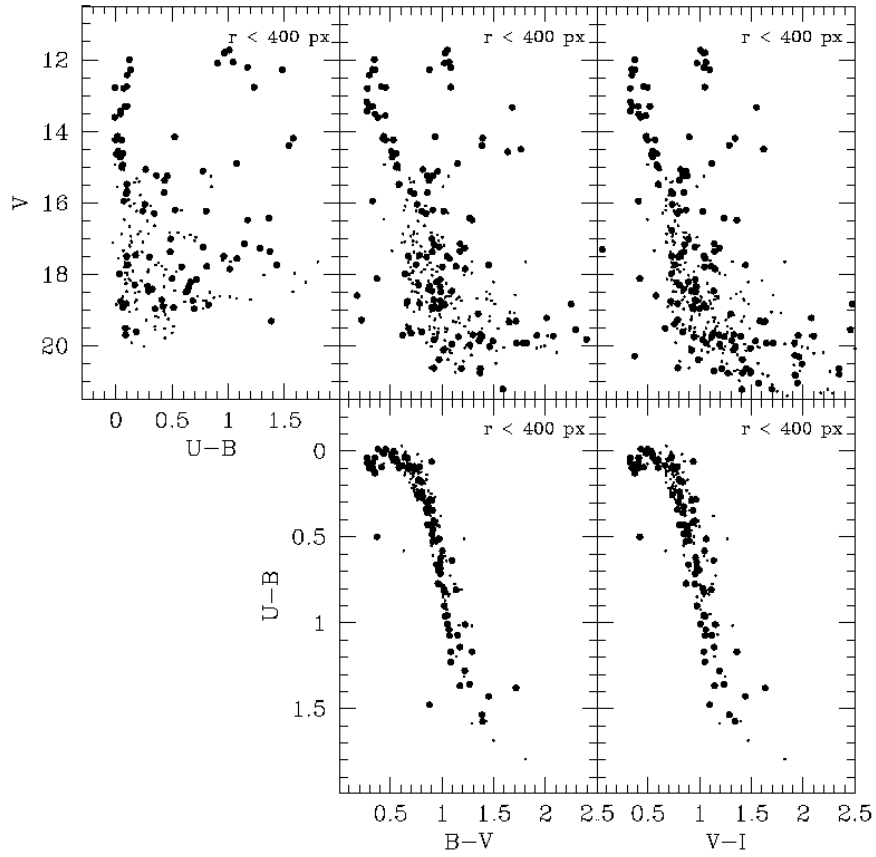


Figure 12. The circular extracted $(V, U - B)$, $(V, B - V)$, and $(V, V - I)$ diagrams (*top*), and circular extracted $(U - B, B - V)$ and $(B - V, V - I)$ diagrams (*bottom*) for the cluster NGC 2479 (dots), compared with those statistically cleaned from field star contamination (filled circles).

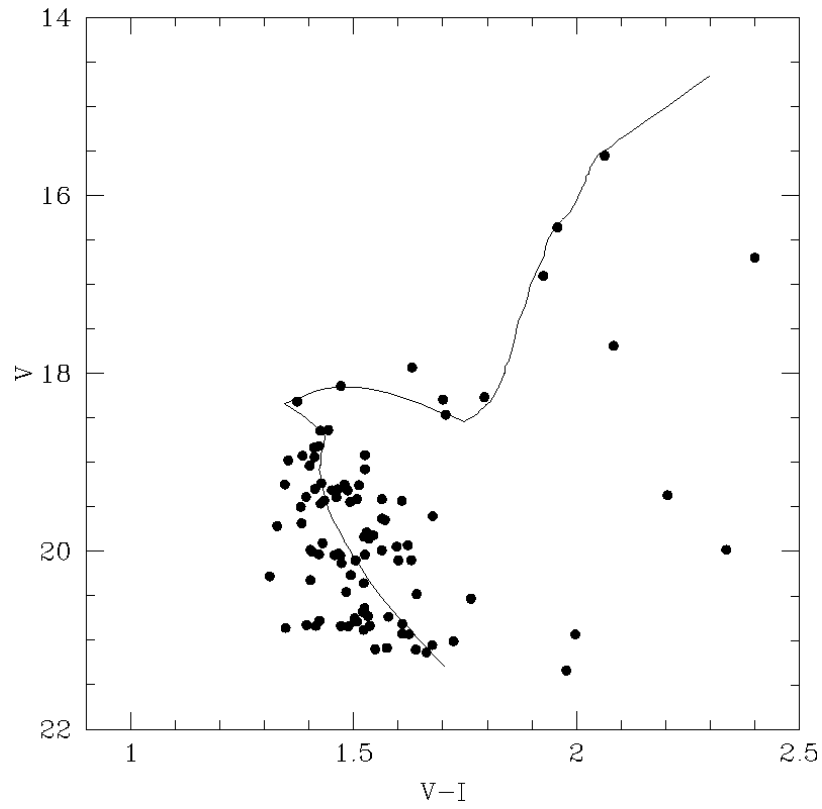


Figure 13. The adopted $(V, V - I)$ diagram for Berkeley 26. The adopted isochrone from Lejeune & Schaerer (2001) are overplotted with solid lines.

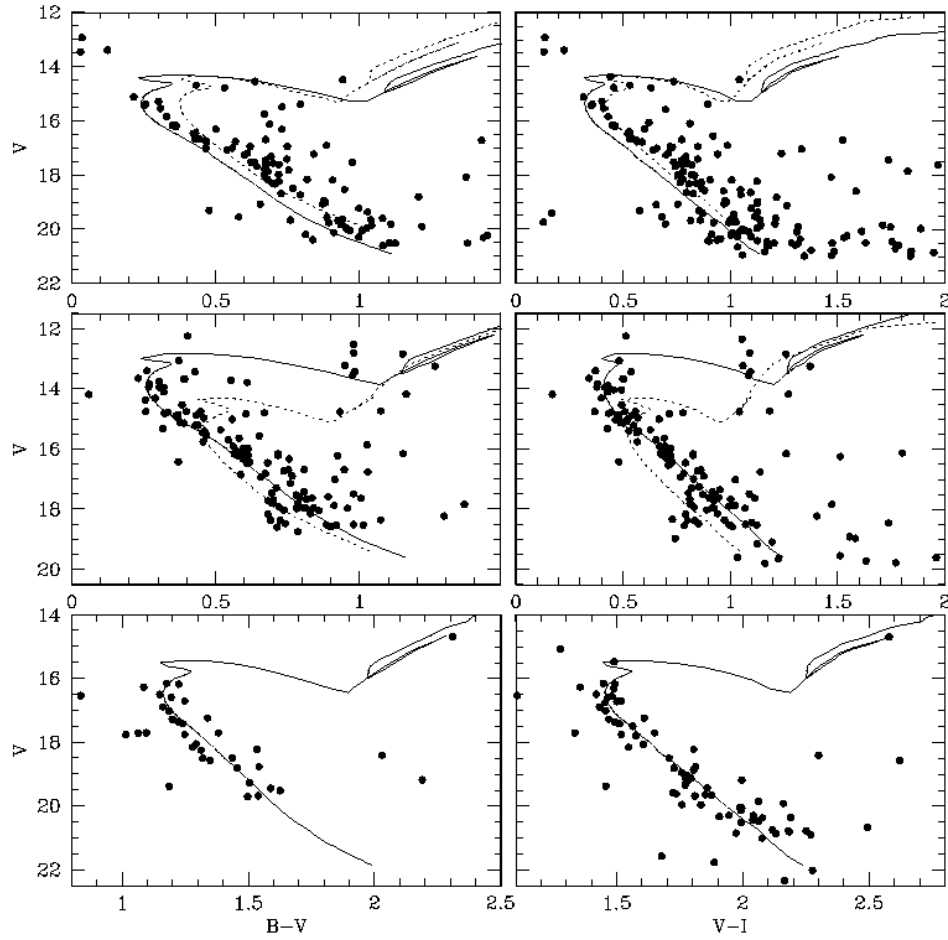


Figure 14. $(V, B - V)$ and $(V, V - I)$ diagrams adopted for Czernik 27 (*top*), Melotte 72 (*middle*) and BH 37 (*bottom*). *Czernik 27*: the isochrones from Lejeune & Schaerer (2001) according to the values published by Kim et al. (2005) and HSM08 (see Sect. 1) are overplotted with solid and dotted lines, respectively. *Melotte 72*: the isochrones from Lejeune & Schaerer (2001) according to the values adopted here and those published by HSM08 (see Sect. 1) are overplotted with solid and dotted lines, respectively. *BH 37*: The adopted isochrone from Lejeune & Schaerer (2001) is overplotted with solid lines.

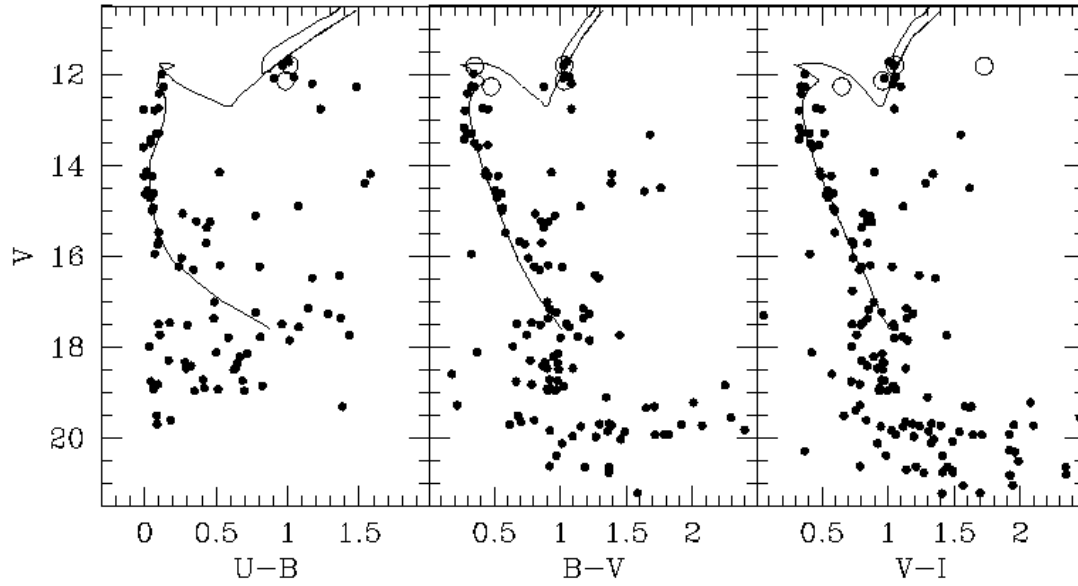


Figure 15. $(V, U - B)$, $(V, B - V)$ and $(V, V - I)$ diagrams adopted for NGC 2479. The adopted isochrones from Lejeune & Schaerer (2001) are overplotted with solid lines. Cluster members according to Kharchenko et al. (2005) are represented by open circles.